PERGAMON

Control Engineering Practice 10 (2002) 925–939

CONTROL ENGINEERING PRACTICE

www.elsevier.com/locate/conengprac

# A new approach to the design of mode switching control in hard disk drive servo systems

V. Venkataramanan[a], Ben M. Chen[a,*], Tong H. Lee[a], Guoxiao Guo[b]

[a] *Department of Electrical and Computer Engineering, National University of Singapore, Singapore 117576, Singapore*
[b] *Data Storage Institute, Engineering Drive 1, Singapore 117608, Singapore*

Received 8 January 2001; accepted 7 December 2001

**Abstract**

In a modern large-capacity magnetic hard disk drive (HDD), both fast track seeking and perfect positioning of the read/write head are required. Mode switching control (MSC) approaches are widely used to meet these requirements. This paper proposes a new approach in designing MSC with an application to HDD servo systems. The proposed scheme uses a proximate time-optimal servomechanism in the track seeking mode, and a robust perfect tracking (RPT) controller in the track following mode. Unlike the conventional MSC approaches, the new method does not require an initial value compensation during mode switching. This is because the RPT controller in the second stage is capable of rendering the $L_p$-norm ($1 \leqslant p < \infty$) of the resulting tracking error arbitrarily small in the presence of external disturbances and initial conditions. Simulation and experimental results show that the proposed method improves the seek and settling time by about 10% over the conventional approaches. 

*Keywords:* Hard disk drives; Servo systems; Mode switching control; Target tracking; Robust control

## 1. Introduction

The prevalent trend in hard disk design is towards smaller hard disks with increasingly larger capacities. This implies that the track width has to be smaller leading to lower error tolerance in the positioning of the head. The controller for track following has to achieve tighter regulation in the control of the servomechanism. Basically, the servo system of a hard disk drive (HDD) can be divided into three stages, i.e., the track seeking, track settling and track following stages. Current HDDs use a combination of classical control techniques, such as proximate time optimal control technique in the tracking seeking stage, and lead-lag compensators, PID compensators in the track following stage, plus some notch filters to reduce the effects of high-frequency resonant modes (see, e.g., Franklin, Powell, & Workman, 1998; Fujimoto, Hori, Yarnaguchi, & Nakagawa, 2000; Goh, Li, Chen, Lee, & Huang, 2001; Gu & Tomizuka, 2000; Hara, Hara, Yi, & Tomizuka, 1999; Huang, Messner, & Steele, 1997; Ishikawa & Tomizuka, 1998; Iwashiro, Yatsu, & Suzuki, 1999; Yamaguchi, Soyama, Hosokawa, Tsuneta, & Hirai, 1996; and references cited therein). These classical methods can no longer meet the demand for HDDs of higher performance. Thus, many control approaches have been tried, such as the linear quadratic Gaussian (LQG) with loop transfer recovery (LTR) approach (see, e.g., Chang & Ho, 1999; Hanselmann & Engelke, 1988; Weerasooriya & Phan, 1995), and adaptive control (see, e.g., Chen, Guo, Huang, & Low, 1998; Workman, 1987) and so on. Although much work has been done to date, more studies need to be conducted to use more control methods to achieve better performance.

In the conventional mode switching control (MSC), the track seeking mode is switched to track following mode under certain conditions. One of the design problems for MSC is the method of switching between controllers. This design problem has not yet been completely resolved, and many heuristic approaches have been tried so far (see, e.g., Yamaguchi, Numasato, & Hirai, 1998). Several methods were proposed for mode switching from one controller to another. Yamaguchi et al. (1996), proposed a method called initial value compensation to reduce the impact of the

*Corresponding author. Tel.: +65-874-2289; fax: +65-779-1103.
*E-mail address:* bmchen@nus.edu.sg (B.M. Chen).

0967-0661/02/$ - see front matter 
PII: S0967-0661(02)00037-0

initial values during mode switching of controllers on the servo performance. Here the initial value means the values of the states during mode switching. However, the robust perfect tracking (RPT) controllers developed by Chen (2000) have enough robustness against external disturbances and are independent of initial values. It is capable of rendering the $L_p$-norm ($1 \leqslant p < \infty$) of the resulting tracking error arbitrarily small for any initial conditions. Hence, the use of these controllers during mode switching eliminates the need for initial value compensation. In this paper, such a controller is used in track following mode to follow the track precisely against various disturbances and plant uncertainty at high frequency. We propose in this paper a new MSC design, which uses a proximate time-optimal servomechanism (PTOS) controller for track seeking, and an RPT controller for track following. These controllers are combined through a suitable mode switching condition.

This paper first briefly describes a head-positioning system of disk drives. Also, a plant model is derived to implement the proposed method. This is done in Section 2. Section 3 gives the main theoretical framework of the paper. In particular, Sections 3.1 and 3.2 recall the design procedures of the PTOS and RPT techniques, whereas in Section 3.3, the MSC technique is proposed together with a detailed derivation of a set of mode switching conditions. The application of these controllers to an HDD is given in Section 4 and the simulation and experimental results are reported in Section 5. Finally, the concluding remarks are drawn in Section 6.

## 2. An HDD

Fig. 1 shows a typical HDD with a voice-coil motor (VCM) actuator servo system. On the surface of a disk, there are thousands of data tracks. A magnetic head is supported by a suspension and a carriage, and it is suspended several microinches above the disk surface. The VCM actuator initiates the carriage and moves the head to a desired track. The mechanical part of the plant, that is, the controlled object, consists of the VCM, the carriage, the suspension, and the heads. The controlled variable is the relative head position. The control input $u$ is a voltage to a current amplifier for the VCM and the measurement output $y$ is the head position in tracks. The frequency response of a commercially available HDD servo system from $u$ to $y$ is shown as a solid line in Fig. 2. This drive will be used in our experimental test. It is quite conventional to approximate the dynamics of the VCM actuator by a second-order state space model as

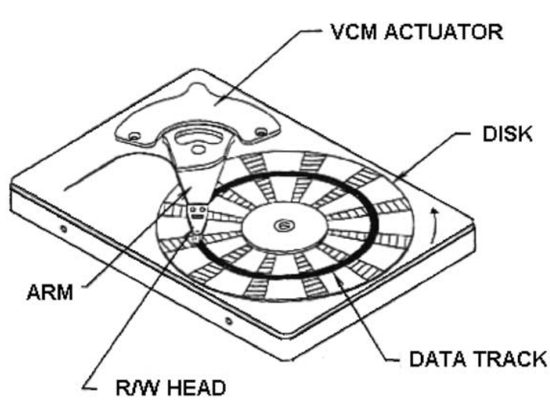


Fig. 1. A hard disk drive with a VCM actuator servo system.

$$\dot{x} = Ax + Bu = \begin{bmatrix} 0 & 1 \\ 0 & 0 \end{bmatrix} x + \begin{bmatrix} 0 \\ a \end{bmatrix} u, \quad x = \begin{pmatrix} y \\ v, \end{pmatrix}, \tag{1}$$

where $x$ is the state, which consists of the displacement $y$ (in micrometer) and the velocity $v$ of the [read/write] (R/W) head; $u$ is the control input (in V) constrained by

$$|u(t)| \leqslant u_{\max} \tag{2}$$

and $a = K_t/J_a$ is the acceleration constant, with $K_t$ being the torque constant and $J_a$ being the moment of inertia of the actuator mass. Thus, the transfer function from $u$ to $y$ of the VCM model can be written as

$$G_{v1}(s) = \frac{a}{s^2}. \tag{3}$$

The frequency response shows that the servo system has many mechanical resonance frequencies over 1 kHz. In general, it is difficult to model these high-frequency modes exactly. However, if we only consider the first dominating resonance frequency, a more realistic model for the VCM actuator should be given as

$$G_v(s) = \frac{a}{s^2} \frac{\omega_n^2}{s^2 + 2\zeta\omega_n s + \omega_n^2}, \tag{4}$$

where $\omega_n$ corresponds to the resonance frequency and $\zeta$ is the associated damping coefficient. To design and implement the proposed controller, an actual HDD is taken and the model is identified through a series of frequency response tests. Fig. 2 shows the frequency response of a Maxtor HDD (Model 51536U3). It is obtained using a laser doppler vibrometer (LDV) and an HP make dynamic signal analyzer (HP35670A). Using the measured data from the actual system (see, Fig. 2), and the algorithms of Eykhoff (1981) and Wang, Yuan, Chen, and Lee (1998), we obtain a fourth-order model for the HDD actuator as

$$G_v(s) = \frac{6.4013 \times 10^7}{s^2} \times \frac{2.467 \times 10^8}{s^2 + 2.513 \times 10^3 s + 2.467 \times 10^8}. \tag{5}$$

This model will be used throughout the rest of the paper in designing appropriate controllers and in simulation.

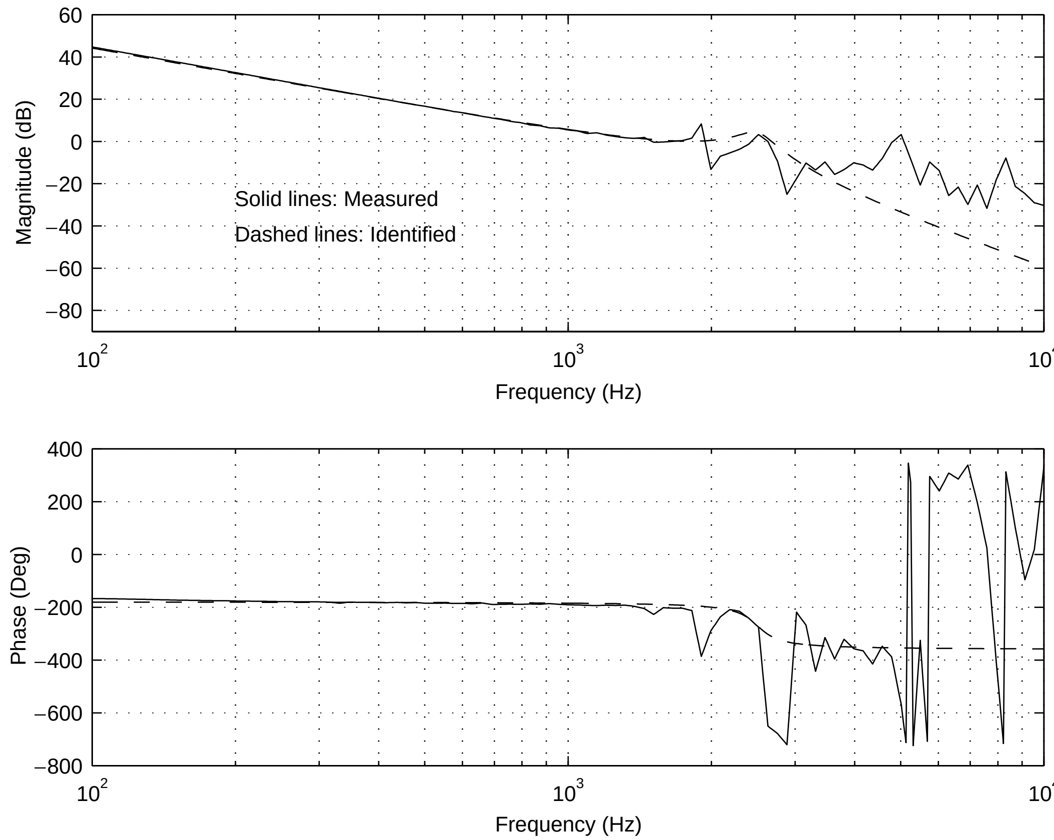


Fig. 2. Frequency response characteristics of HDD.

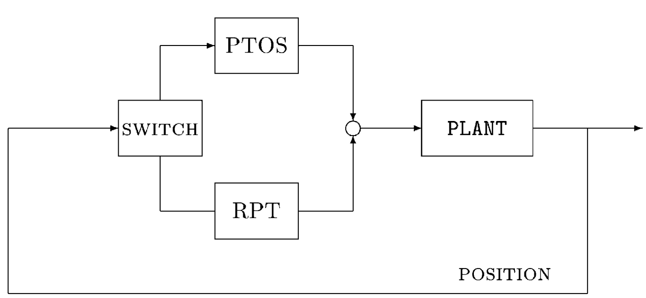


Fig. 3. Basic schematic diagram of MSC.

## 3. Mode switching control

In HDD servo systems, in order to achieve both high-speed track seeking and highly accurate head positioning, multimode control designs are widely used. The two commonly used multimode control designs are MSC and sliding mode control. Both control techniques in fact belong to the category of variable structure control. That is, the control is switched between two or more different controllers to achieve the two conflicting requirements. As mentioned earlier in this paper, we will propose an MSC control in which the seeking mode is controlled by a PTOS and the track following mode is controlled by an RPT controller.

The MSC is a type of variable-structure control system (Itkis, 1976), but the switching is in only one direction. Fig. 3 shows a basic schematic diagram of MSC. There are a track seeking mode and a track following mode. Each servo mode can be designed independently. Thus, the main issue in MSC is the design of switching mechanism.

This design problem has not yet been completely resolved, and many heuristic approaches have been tried so far (see, e.g., Yamaguchi et al., 1998). Several methods were proposed for mode switching from one controller to another. In Yamaguchi et al. (1996), a method called initial value compensation is proposed. Note that, when the switch is transferred from the track seeking mode to the track following mode, the final states of the track seeking stage become the initial states for the track following stage, and hence affect the settling performance of track following mode. In order to reduce the impact of these initial values during mode switching, some compensation must be worked out. The RPT controllers developed by Chen (2000) and Liu, Chen, and Lin (2001) have enough robustness against plant variations and are actually independent of initial values. The use of these controllers in track following mode would eliminate the need for initial value compensation during mode switching. Moreover, the

RPT controllers in a track following servo have been proven by Goh et al. (2001) to be robust against resonance mode changes from disk to disk and work well against runout disturbances.

### 3.1. The PTOS controller

Track seeking is a time-optimal control problem. In this subsection, we recall the conventional PTOS design for the following continuous-time model of the rigid body mechanical dynamics characterized by

$$\dot{x} = \begin{bmatrix} 0 & 1 \\ 0 & 1 \end{bmatrix} x + \begin{bmatrix} 0 \\ a \end{bmatrix} u_{\mathrm{P}}, \tag{6}$$

where $x = [y \;\; v]'$, $y$ is position in tracks, $v$ is velocity of the R/W head. Let $r$ be the desired relative head position in tracks, $e = y - r$ be the position error. The PTOS control is given by (see, Workman, 1987)

$$u_{\mathrm{P}} = u_{\max} \operatorname{sat}\left( \frac{k_2[f(e) - v]}{u_{\max}} \right), \tag{7}$$

where function $f(\cdot)$ is given by

$$f(e) = \begin{cases} \dfrac{k_1}{k_2} e & \text{for } |e| \leqslant y_\ell, \\ \operatorname{sgn}(e) \left[ \sqrt{2 a u_{\max} \alpha |e|} - \dfrac{u_{\max}}{k_2} \right] & \text{for } |e| > y_\ell. \end{cases} \tag{8}$$

Here the constant gains $k_1$ and $k_2$ are determined from the acceleration discount factor $\alpha$ $(0 < \alpha < 1)$, and the closed-loop poles during track following mode with the following constraints (Workman, 1987):

$$k_1 = \frac{u_{\max}}{y_\ell} \quad \text{and} \quad k_2 = \sqrt{\frac{2k_1}{\alpha a}}, \tag{9}$$

where $y_\ell$ is the linear region or the track following region. The schematic diagram of the track seeking controller is shown in Fig. 4.

### 3.2. The RPT controller

The RPT control was proposed by Chen (2000) and Liu et al. (2001). It was successfully applied by Goh et al. (2001) to design an HDD servo system, in which a first-order dynamic measurement feedback controller was carried out to achieve a robust and perfect tracking for any step reference and for arbitrary initial conditions. This controller is theoretically capable of making the $L_p$-norm $(1 \leqslant p < \infty)$ of the resulting tracking error arbitrarily small in the presence of external disturbances. Moreover, these controllers show lower overshoots and higher accuracy. The design procedure of the RPT control is as follows:

Consider a general linear system with external disturbances described by the following state space model $\Sigma$:

$$\dot{x} = A_p x + B_p u_{\mathrm{R}} + E w,$$
$$y = C_1 x + D_1 w,$$
$$h = C_2 x + D_2 u, \tag{10}$$

where $x \in \mathbb{R}^n$ is the state variable of the system, $w \in \mathbb{R}^k$ is the external disturbance, $y \in \mathbb{R}^q$ is the measurement output, and $h \in \mathbb{R}^l$ is the output to be controlled. Then the robust and perfect tracking problem is to design a parameterized controller of the following form $\Sigma_v(\varepsilon)$:

$$\dot{x}_v = A_v(\varepsilon) x_v + B_{vy}(\varepsilon) y + B_{vr}(\varepsilon) r,$$
$$u_{\mathrm{R}} = C_v(\varepsilon) x_v + D_{vy}(\varepsilon) y + D_{vr}(\varepsilon) r, \tag{11}$$

where $x_v \in \mathbb{R}^{n_v}$ is the state variable of the control law, such that the following properties hold:

(1) *Internal stability*: The resulting closed-loop system comprising the system $\Sigma$ of (10) and the control law $\Sigma_v(\varepsilon)$ of (11) is internally stable for all $\varepsilon \in (o, \varepsilon^*]$, where $\varepsilon^*$ is a positive scalar; and
(2) *Robust and perfect tracking*: For any $1 \leqslant p < \infty$, any $w \in L_p$ and any bounded initial condition $x_0$, the resulting tracking error satisfies

$$\|h - r\|_p \to 0, \quad \text{as } \varepsilon \to 0, \tag{12}$$

where obviously $h$ is also a function $\varepsilon$, which can be rewritten as $h(t, \varepsilon)$. The above property implies that the output to be controlled $h(t, \varepsilon)$ is capable of tracking the reference $r(t)$ within no time in the presence of external disturbances and initial conditions.

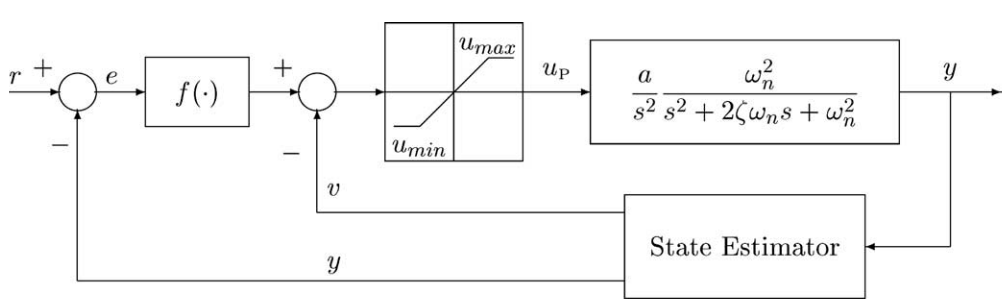


Fig. 4. The track seeking controller.

It was shown in Chen (2000) and Liu et al. (2001) that the above RPT problem with $x(0) = x_0$ and with external disturbance is solvable if the following conditions are satisfied: (1) $(A, B)$ is stabilizable and $(A, C_1)$ is detectable; and (2) the subsystem $(A, B, C_2, D_2)$ is of minimum phase and right invertible.

To solve the RPT problem, we first let

$$r(t) = \begin{bmatrix} \alpha_1 \\ \alpha_2 \\ \vdots \\ \alpha_\ell \end{bmatrix} \cdot 1(t) = \boldsymbol{\alpha} \cdot 1(t), \tag{13}$$

where $1(t)$ is the unit step function, and $\alpha_1, \alpha_2, \ldots, \alpha_\ell$ are the magnitudes of the step functions. Thus, we have

$$\dot{r}(t) = \boldsymbol{\alpha} \cdot \delta(t), \tag{14}$$

where $\delta(t)$ is a unit impulse function. Combining the original system $\Sigma$ of (10) and the reference signal $r(t)$, we obtain an auxiliary system $\Sigma_{\text{aux}}$

$$\dot{\boldsymbol{x}} = \boldsymbol{A}\boldsymbol{x} + \boldsymbol{B}\boldsymbol{u} + \boldsymbol{E}\boldsymbol{w},$$

$$\boldsymbol{y} = \boldsymbol{C}_1\boldsymbol{x} + \boldsymbol{D}_1\boldsymbol{w},$$

$$\boldsymbol{e} = \boldsymbol{C}_2\boldsymbol{x} + \boldsymbol{D}_2\boldsymbol{u}, \tag{15}$$

where

$$\boldsymbol{x} = \begin{pmatrix} r \\ x \end{pmatrix}, \quad \boldsymbol{u} = u, \quad \boldsymbol{w} = \begin{pmatrix} w \\ \boldsymbol{\alpha}\delta(t) \end{pmatrix}, \tag{16}$$

$$\boldsymbol{y} = \begin{pmatrix} r \\ y \end{pmatrix}, \quad \boldsymbol{e} = h - r \tag{17}$$

and

$$\boldsymbol{A} = \begin{bmatrix} 0 & 0 \\ 0 & A \end{bmatrix}, \quad \boldsymbol{B} = \begin{bmatrix} 0 \\ B \end{bmatrix}, \quad \boldsymbol{E} = \begin{bmatrix} 0 & I_\ell \\ E & 0 \end{bmatrix}, \tag{18}$$

$$\boldsymbol{C}_2 = [-I \quad C_2], \quad \boldsymbol{D}_2 = D_2, \tag{19}$$

$$\boldsymbol{C}_1 = \begin{bmatrix} I & 0 \\ 0 & C_1 \end{bmatrix}, \quad \boldsymbol{D}_1 = \begin{bmatrix} 0 & 0 \\ D_1 & 0 \end{bmatrix}. \tag{20}$$

Note that $\boldsymbol{e}(t)$ is the tracking error. The construction algorithm involves two step main stages (see, e.g., Chen, 2000): In the first stage, a static state feedback law for $\Sigma_{\text{aux}}$ of (15), which would solve the RPT problem for the case when $y = x$, i.e., all the states of $\Sigma$ are available for measurement, is designed. Then, in the second stage, a reduced order measurement feedback control law that would recover the performance of the static state feedback law designed in the first stage is obtained. A simplified procedure of the RPT design for HDD servo systems can also be found in Goh et al. (2001).

### 3.3. Mode switching conditions

The MSC law that combines the PTOS and RPT controllers takes the following simple form:

$$u = \begin{cases} u_{\text{P}}, & t < t_1, \\ u_{\text{R}}, & t \geqslant t_1, \end{cases} \tag{21}$$

where $u_{\text{P}}$ is the control generated by the PTOS controller and is given as in (7), and $u_{\text{R}}$ is the control generated by the reduced order RPT controller as given in (10). Furthermore, $t_1$, the time that MSC switches from one mode to the other, will be presented later together with the stability analysis of the closed-loop system comprising the given plant and the MSC control law.

Let us move to show the stability of the MSC and give a set of conditions for mode switching. First of all, we rewrite the given system (1) as follows:

$$\begin{pmatrix} \dot{e} \\ \dot{v} \end{pmatrix} = \begin{bmatrix} 0 & -1 \\ 0 & 0 \end{bmatrix} \begin{pmatrix} e \\ v \end{pmatrix} + \begin{bmatrix} 0 \\ a \end{bmatrix} u := A_{\text{P}} x_{\text{P}} + B_{\text{P}} u,$$
$$a > 0, \tag{22}$$

where $e = r - y$ is the tracking error with $r$ being the target reference; $y$ is the displacement of an HDD R/W head and $v$ is its velocity. Recall the PTOS control law:

$$u_{\text{P}} = u_{\max} \operatorname{sat}\left[\frac{k_2}{u_{\max}}(f(e) - v)\right], \tag{23}$$

where the $u_{\max}$ used throughout this section has a saturation level equal to unity; the function $f(\cdot)$ and the feedback gain $k_2$ are as defined in the previous subsection. It has been shown in Workman (1987) that the PTOS control law will yield an asymptotically stable closed-loop system provided that the following conditions are satisfied:

(1) $ak_2 > 0$;
(2) $f(0) = 0$;
(3) $f(e)e > 0$, for any nonzero $e$;
(4) $\lim_{e \to \infty} \int_0^e f(\delta)\, d\delta = \infty$;
(5) $\dot{f}(e)$ exists everywhere; and
(6) for any $e$, $u_{\max}[-a + 1/k_2]\dot{f}(e) < -\dot{f}(e)f(e) < u_{\max}[a - (1/k_2)\dot{f}(e)]$.

Generally, as the velocity is not measurable, the PTOS control law will have to be modified as follows if it is to be implemented in a real system:

$$u_{\text{P}} = u_{\max} \operatorname{sat}\left[\frac{k_2}{u_{\max}}(f(e) - \hat{v})\right],$$

$$\dot{z} = -\kappa z + \kappa^2 e + a u_{\text{P}},$$

$$\hat{v} = z - \kappa e, \tag{24}$$

where $\kappa$ is the estimator feedback gain, and $z$ is the estimator state. Next, we let $\tilde{z} = z - v - \kappa e$. Then, the dynamics of the closed-loop system with the above control law can be written as

$$\dot{e} = -v,$$

$$\dot{v} = a u_{\max}\,\mathrm{sat}\left[\frac{k_2}{u_{\max}}(f(e) - \tilde{z} - v)\right],$$

$$\dot{\tilde{z}} = -\kappa\tilde{z}. \tag{25}$$

It can be shown that the closed-loop system comprising the given plant and the modified PTOS control law, in which the velocity is replaced by the above estimation, is asymptotically stable, if conditions (1)–(5) above are satisfied and condition (6) is replaced by

$$a > \frac{1}{k_2}\dot{f}(e) > 0 \tag{26}$$

and

$$|\dot{f}(e)f(e)| < u_{\max}\left[a - \frac{1}{k_2}\dot{f}(e)\right] - [\kappa + \dot{f}(e)]\cdot|\tilde{z}(0)|. \tag{27}$$

We can show that, under these new conditions, the closed loop is stable for the case when the control input is saturated, i.e., $|k_2[f(e) - (z - \kappa e)]| > u_{\max}$. For the case when $|k_2[f(e) - (z - \kappa e)]| \leqslant u_{\max}$, the closed-loop system in (25) can be written as

$$\dot{e} = -v,$$

$$\dot{v} = a k_2[f(e) - \tilde{z} - v],$$

$$\dot{\tilde{z}} = -\kappa\tilde{z}. \tag{28}$$

Following the result of LaSalle (1961), we propose the following Lyapunov function for the system in (28):

$$V_{\mathrm{P}} = \frac{v^2}{2k_2 a} + \int_0^e f(\delta)\,\mathrm{d}\delta + \frac{p_z}{2}\tilde{z}^2, \tag{29}$$

where $p_z > 0$ is a scalar constant. The derivative of the above Lyapunov function is given by

$$\dot{V}_{\mathrm{P}} = -\left(v + \frac{\tilde{z}}{2}\right)^2 - \tilde{z}^2\left(p_z\kappa - \frac{1}{4}\right). \tag{30}$$

The last term is negative for all $p_z > 1/4\kappa$. Thus, under this choice of $p_z$, $\dot{V}_{\mathrm{P}} \leqslant 0$. It follows from LaSalle's Theorem (LaSalle, 1961) that the closed-loop system comprising the PTOS control law with the estimated velocity and the given plant is asymptotically stable.

It is pretty obvious that the closed-loop system comprising the given plant in (22) and the reduced order RPT control law of (11) is asymptotically stable when the control input is not saturated. For completeness, and for the analysis of the overall closed-loop system with the MSC scheme, we proceed to investigate the closed-loop system comprising the plant and the RPT controller, which can be written as

$$\dot{z} = -\kappa z + \kappa^2 e + a u_{\max}\,\mathrm{sat}\left(\frac{u_{\mathrm{R}}}{u_{\max}}\right),$$

$$u_{\mathrm{R}} = (f_1 - \kappa f_2)e + f_2 z, \tag{31}$$

where $\kappa$ is again the reduced order observer gain, which is selected to be exactly the same as that used for the velocity estimation in the PTOS, and $F = [f_1 \quad f_2]$ is the feedback gain obtained using the RPT technique of Section 3.2. Again, let $\tilde{z} = z - v - \kappa e$ and rewrite the RPT control law as

$$u_{\mathrm{R}} = [f_1 \quad f_2]\begin{pmatrix} e \\ v \end{pmatrix} + f_2\tilde{z} = F x_{\mathrm{P}} + f_2\tilde{z}. \tag{32}$$

Let $W_x \in \mathbb{R}^{2\times 2}$ be a positive definite matrix and solve the following Lyapunov equation:

$$(A_{\mathrm{P}} + B_{\mathrm{P}}F)'P_x + P_x(A_{\mathrm{P}} + B_{\mathrm{P}}F) = -W_x \tag{33}$$

for $P_x > 0$. Such a $P_x$ always exists as $A_{\mathrm{P}} + B_{\mathrm{P}}F$ is stable. Next, let

$$w_z > \max\left\{\frac{1}{2}, f_2 B_{\mathrm{P}}' P_x W_x^{-1} P_x B_{\mathrm{P}} f_2\right\} > 0 \tag{34}$$

and

$$p_z = \frac{w_z}{2\kappa} > \frac{1}{4\kappa} > 0. \tag{35}$$

Then, we define a set

$$\boldsymbol{X} := \left\{\begin{pmatrix} x \\ z \end{pmatrix} : \begin{pmatrix} x \\ z \end{pmatrix}'\begin{bmatrix} P_x & 0 \\ 0 & p_z \end{bmatrix}\begin{pmatrix} x \\ z \end{pmatrix} \leqslant c\right\}, \tag{36}$$

where $c > 0$ is the largest positive value such that

$$\begin{pmatrix} x \\ z \end{pmatrix} \in \boldsymbol{X} \Rightarrow \left|\begin{bmatrix} F & f_2 \end{bmatrix}\begin{pmatrix} x \\ z \end{pmatrix}\right| \leqslant u_{\max}. \tag{37}$$

For all

$$\begin{pmatrix} x_{\mathrm{P}} \\ z \end{pmatrix} \in \boldsymbol{X} \tag{38}$$

the resulting closed-loop system can then be written as

$$\begin{pmatrix} \dot{x}_{\mathrm{P}} \\ \dot{\tilde{z}} \end{pmatrix} = \begin{bmatrix} A_{\mathrm{P}} + B_{\mathrm{P}}F & B_{\mathrm{P}}f_2 \\ 0 & -\kappa \end{bmatrix}\begin{pmatrix} x_{\mathrm{P}} \\ \tilde{z}. \end{pmatrix}. \tag{39}$$

Define a Lyapunov function,

$$V_{\mathrm{R}} = \begin{pmatrix} x_{\mathrm{P}} \\ \tilde{z}' \end{pmatrix}\begin{bmatrix} P_x & 0 \\ 0 & p_z \end{bmatrix}\begin{pmatrix} x_{\mathrm{P}} \\ \tilde{z} \end{pmatrix} \tag{40}$$

and evaluate its derivative along the trajectories of the closed-loop system in (39), i.e.,

$$\dot{V}_{\mathrm{R}} = \begin{pmatrix} x_{\mathrm{P}} \\ \tilde{z}' \end{pmatrix}\begin{bmatrix} -W_x & P_x B_{\mathrm{P}} f_2 \\ f_2 B_{\mathrm{P}}' P_x & -w_z \end{bmatrix}\begin{pmatrix} x_{\mathrm{P}} \\ \tilde{z} \end{pmatrix},$$

$$= \begin{pmatrix} \hat{x} \\ \tilde{z}' \end{pmatrix}\begin{bmatrix} -W_x & 0 \\ 0 & -\tilde{w}_z \end{bmatrix}\begin{pmatrix} \hat{x} \\ \tilde{z} \end{pmatrix} \leqslant 0, \tag{41}$$

where

$$\hat{x} = x_{\mathrm{P}} - W_x^{-1}P_x B_p f_2\tilde{z},$$

$$\tilde{w}_z = w_z - f_2' B_{\mathrm{v}}' P_x W_x^{-1} P_x B_p f_2 > 0. \tag{42}$$

This shows that all trajectories of (39) starting from $\boldsymbol{X}$ will remain there and converge asymptotically to zero. Hence, the closed-loop system comprising the plant and the reduced order RPT control law is asymptotically stable provided that the control input is not saturated.

Next, we re-express (29) using the Taylor expansion as follows:

$$V_{\mathrm{P}} = \frac{v^2}{2k_2 a} + \frac{\dot{f}(\tau)}{2} e^2 + \frac{p_z}{2} \tilde{z}^2 = \begin{pmatrix} e \\ v \\ \tilde{z}' \end{pmatrix} \begin{bmatrix} \frac{\dot{f}(\tau)}{2} & 0 & 0 \\ 0 & \frac{1}{2ak_2} & 0 \\ 0 & 0 & \frac{p_z}{2} \end{bmatrix} \begin{pmatrix} e \\ v \\ \tilde{z} \end{pmatrix},$$

where $\tau$ is an appropriate scalar between 0 and $e$. Let

$$\sigma = \min\left\{ \frac{\dot{f}(\tau)}{2}, \frac{1}{2ak_2}, \frac{p_z}{2} \right\} \Big/ \max\{\lambda_{\max}(P_x), p_z\}. \tag{43}$$

The MSC scheme can be obtained as follows:

$$u(t) = \begin{cases} u_{\mathrm{P}}, & t < t_1, \\ u_{\mathrm{R}}, & t \geqslant t_1, \end{cases} \tag{44}$$

where $t_1$ is such that

$$\begin{pmatrix} x_{\mathrm{P}}(t_1) \\ z(t_1) \end{pmatrix} \in \boldsymbol{X} \quad \text{and} \quad |e(t_1)| < y_\ell \tag{45}$$

and where $y_\ell$ is the size of the linear region of the PTOS control law. The Lyapunov function for the overall closed-loop system can be chosen as

$$V = V_{\mathrm{P}}[1 - 1(t - t_1)] + \sigma V_{\mathrm{R}} 1(t - t_1), \tag{46}$$

where $1(t)$ is the unit step function. It is simple to verify that

$$\dot{V} = \dot{V}_{\mathrm{P}}[1 - 1(t - t_1)] + \sigma \dot{V}_{\mathrm{R}} 1(t - t_1) + (\sigma V_{\mathrm{R}} - V_{\mathrm{P}})\delta(t - t_1). \tag{47}$$

It has already been proved that the derivatives of the functions $V_{\mathrm{P}}$ and $V_{\mathrm{R}}$ are negative definite. The last term is always negative in view of the definition of $\sigma$ in (43). Hence, $\dot{V} \leqslant 0$ and the resulting closed-loop system comprising the given plant and the MSC law is asymptotically stable.

## 4. An HDD servo system design

The HDD servomechanism model considered is a double integrator with one resonance mode as given in (5). We now move to find the control law for each mode of operation based on the design procedures discussed in the previous section. For the track seeking mode, the first step in forming a PTOS law is to find the gains $k_1$ and $k_2$ based on the design specifications. From the physical properties of the HDD system, we found that it is reasonable to choose a set of closed-loop poles with a natural frequency of $1.0681 \times 10^3$ rad/s, i.e., 170 Hz, and the damping factor of 0.898 so as to have the acceleration discount factor $\alpha = 0.62$. We would like to note that these parameters are selected for the PTOS design so that it is implementable for our HDD model given by (5). Thus, the desired closed-loop poles are

$$s_{1,2} = -2.277 \times 10^3 \pm j2.163 \times 10^3. \tag{48}$$

Using $m$-function `acker` in MATLAB, we obtain the following feedback gains:

$$k_1 = 0.0178 \quad \text{and} \quad k_2 = 2.997 \times 10^{-5} \tag{49}$$

and the length of the linear region in PTOS $y_\ell = 168.318$ μm. Thus, the PTOS control law for our disk drive is given by

$$u_{\mathrm{P}} = u_{\max} \operatorname{sat}\left( \frac{k_2[f_p(e) - v]}{u_{\max}} \right), \tag{50}$$

where

$$f_p(e) = \begin{cases} \dfrac{k_1}{k_2} e, & \text{for } |e| \leqslant y_\ell, \\ \operatorname{sgn}(e)\left[ \sqrt{2u_{\max} a\alpha |e|} - \dfrac{u_{\max}}{k_2} \right], & \text{for } |e| > y_\ell \end{cases} \tag{51}$$

with

$$a = 6.4013 \times 10^7, \quad k_1 = 0.0178, \quad k_2 = 2.997 \times 10^{-5} \tag{52}$$

and

$$y_\ell = 168.318, \quad \alpha = 0.62. \tag{53}$$

The implementation of such a controller requires an estimation of the VCM actuator velocity (with the estimator pole being placed at $-4000$). In the track following mode, we consider the following specifications:

(1) The control input should not exceed $\pm 3$ V due to physical constraints on the actual VCM actuator.
(2) The overshoot and undershoot of the step response should be kept $< 5\%$ as the R/W head can start to read or write within $\pm 5\%$ of the target.
(3) The 5% settling time in the step response should be as fast as possible.

Let us consider the simplified model without the resonance mode, i.e., the second-order model given by (1), and form a corresponding auxiliary system as in the format of (15):

$$\dot{\boldsymbol{x}} = \begin{bmatrix} 0 & 0 & 0 \\ 0 & 0 & 1 \\ 0 & 0 & 0 \end{bmatrix} \boldsymbol{x} + \begin{bmatrix} 0 \\ 0 \\ 6.4013 \times 10^7 \end{bmatrix} u + \begin{bmatrix} 1 \\ 0 \\ 0 \end{bmatrix} \boldsymbol{w},$$

$$\boldsymbol{y} = \begin{bmatrix} 1 & 0 & 0 \\ 0 & 1 & 0 \end{bmatrix} \boldsymbol{x} + \begin{bmatrix} 0 \\ 0 \end{bmatrix} \boldsymbol{w},$$

$$e = [-1 \quad 1 \quad 0]\boldsymbol{x} + 0u, \tag{54}$$

where

$$\boldsymbol{x} = \begin{pmatrix} r \\ x \end{pmatrix}, \quad \boldsymbol{w} = \alpha \cdot \delta(t), \quad \boldsymbol{y} = \begin{pmatrix} r \\ y \end{pmatrix}, \quad e = h - r. \tag{55}$$

Following the construction algorithm for the RPT controllers, we obtain a parameterized first-order measurement feedback control law

$$\dot{v} = A_{\mathrm{RC}}(\varepsilon)v + B_{\mathrm{RC}}(\varepsilon)\begin{pmatrix} r \\ y \end{pmatrix},$$
$$u = C_{\mathrm{RC}}(\varepsilon)v + D_{\mathrm{RC}}(\varepsilon)\begin{pmatrix} r \\ y \end{pmatrix} \tag{56}$$

with

$$A_{\mathrm{RC}}(\varepsilon) = -8410.8/\varepsilon,$$
$$B_{\mathrm{RC}}(\varepsilon) = \frac{1}{\varepsilon^2}[7.9952 \times 10^6 \quad -4.1637 \times 10^7],$$
$$C_{\mathrm{RC}}(\varepsilon) = -6.8905 \times 10^{-5}/\varepsilon,$$
$$D_{\mathrm{RC}}(\varepsilon) = \frac{1}{\varepsilon^2}[0.1249 \quad -0.4005]. \tag{57}$$

After several trials, we find that the controller parameters of (57) with $\varepsilon = 1$ will give us a satisfactory performance. The mode switching conditions as derived in Section 3.3 can be determined as $|e(t_1)| \leqslant 2\ \mu\mathrm{m} < y_\ell = 168.318\ \mu\mathrm{m}$ and $|v(t_1)| \leqslant 2703\ \mu\mathrm{m/s}$. We select an MSC law,

$$u = \begin{cases} u_{\mathrm{P}}, & t < t_1, \\ u_{\mathrm{R}}, & t \geqslant t_1 \end{cases} \tag{58}$$

in which $t_1$ is chosen such that

$$|y(t_1) - r| = 2\ \mu\mathrm{m} \quad \text{and} \quad |v(t_1)| \leqslant 2703\ \mu\mathrm{m/s}. \tag{59}$$

It can be shown that the overall closed-loop system comprising the given HDD and the MSC control law is indeed asymptotically stable. We will compare the performance of this MSC controller with that of the PTOS controller given by (50).

## 5. Simulation and experimental results

The proposed controller given by (58) has been implemented on the actual HDD identified in Section 2. The results are compared with those of the conventional PTOS controller given by (50). In particular, we will study the following issues:

(1) track seeking and following test;
(2) runout disturbance test; and
(3) position error signal (PES) test.

All simulation results presented in this section are done using Simulink in Matlab and all implementation results are carried out using own experimental setup. Our controllers are implemented using a dSPACE DSP with a sampling rate of 10 kHz. The R/W head position is measured using an LDV.

### 5.1. Track seeking and following test

In our simulation and implementation, we use a track pitch of 1 μm for the HDD. The settling time in simulation is defined as the total time required for the R/W head to move from its initial position to within 5% of track pitch around the target track, which is the region the servo system can start to read or write data. In what follows, we present results for two selected track seek lengths (SL), i.e., SL = 1 and 50 μm. Unfortunately, due to the capacity of our LDV, which is used to measure the displacement of the R/W head of the VCM actuator, the absolute errors of our implementation results given below are 0.05 and 0.1 μm for SL = 1 and 50 μm, respectively. As such, the settling time for both simulation and implementation results is re-defined as the total time required for the R/W head to move from its initial position to the entrance of the region of the final target with plus and minus of the respective absolute error. This is the best we can do with our current experimental setup. Nonetheless, the results we have obtained here should be sufficient enough to illustrate our design ideas and philosophy.

The simulation results for SL = 1 and 50 μm, respectively, are shown in Figs. 5 and 6 and the corresponding implementation results are shown in Figs. 7 and 8. The results in Figs. 5 and 6 are obtained using Simulink while those in Figs. 7 and 8 are experimental results obtained from the actual system.

We now summarize the overall results on settling times and percentages of improvement in Table 1. Clearly, the simulation and implementation results show that the servo system with the proposed MSC controller yields a better performance.

### 5.2. Runout disturbance test

The disturbances in a real HDD are usually considered as a lumped disturbance at the plant output, also known as runouts. Repeatable runouts (RRO) and nonrepeatable runouts (NRRO) are the major sources of track following errors. RRO is caused by the rotation of the spindle motor and consists of frequencies that are multiples of the spindle frequency. NRRO can be perceived as coming from three main sources: vibration shocks, mechanical disturbance and electrical noise. Static force due to flex cable bias, pivot-bearing friction and windage are all components of the vibration shock disturbances. Mechanical disturbances include spindle motor variations, disk flutter and slider vibrations. Electrical noises include quantization errors, media noise, servo demodulator noise and power amplifier

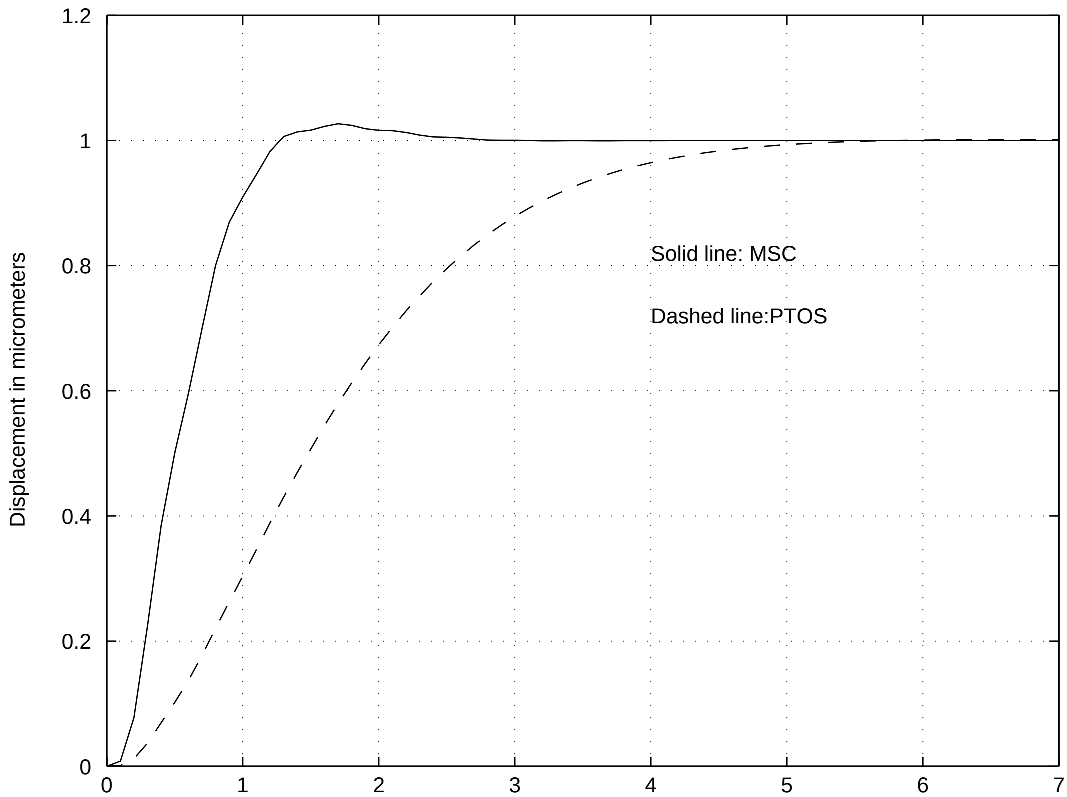


(a)

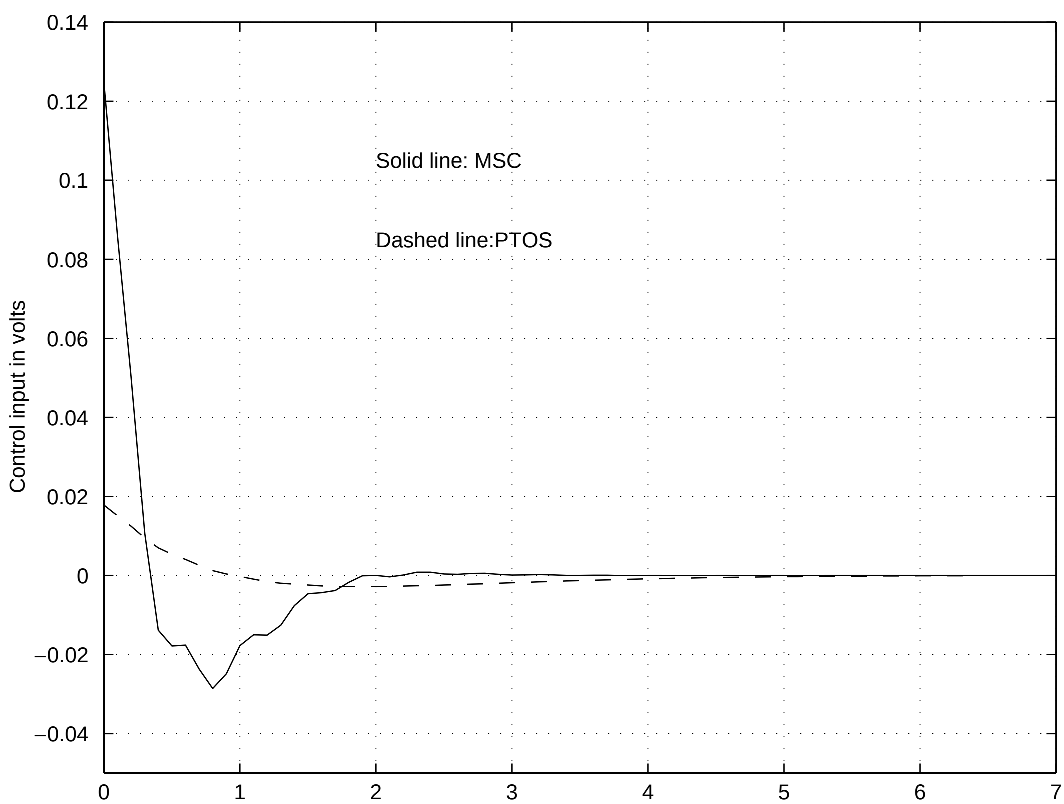


(b)

Fig. 5. Simulation results: response and control for 1 μm displacement: (a) Output responses; (b) control signals.

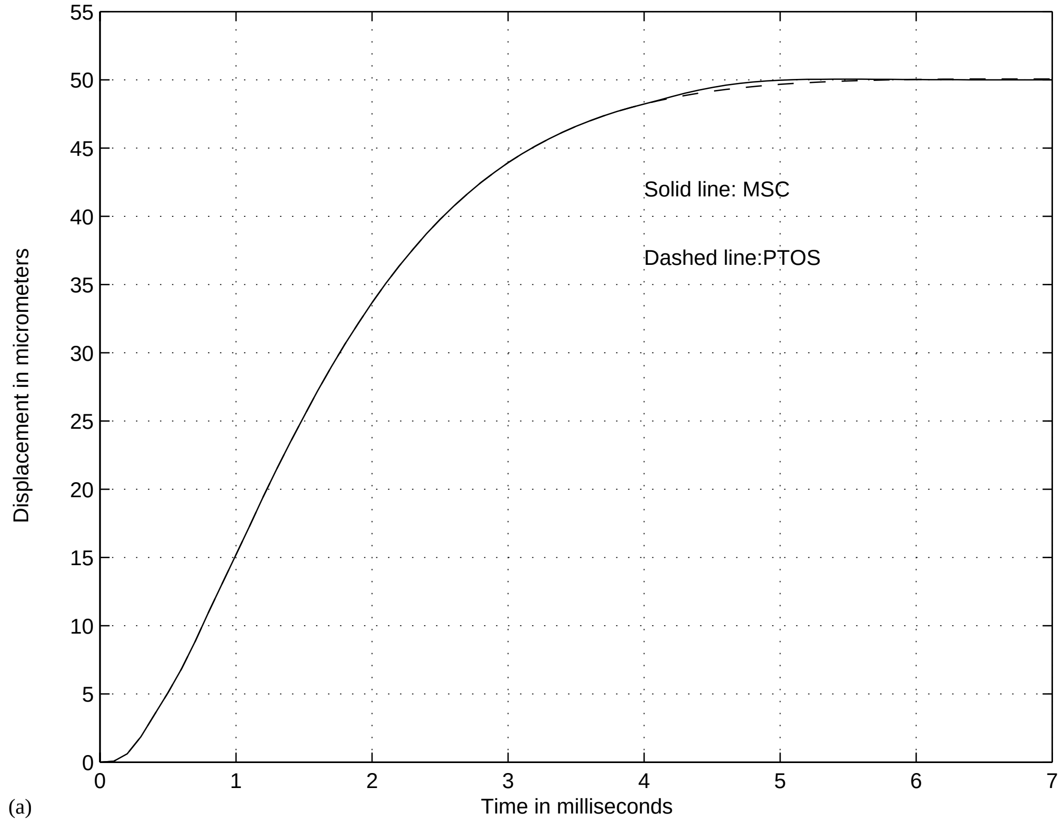

(a)

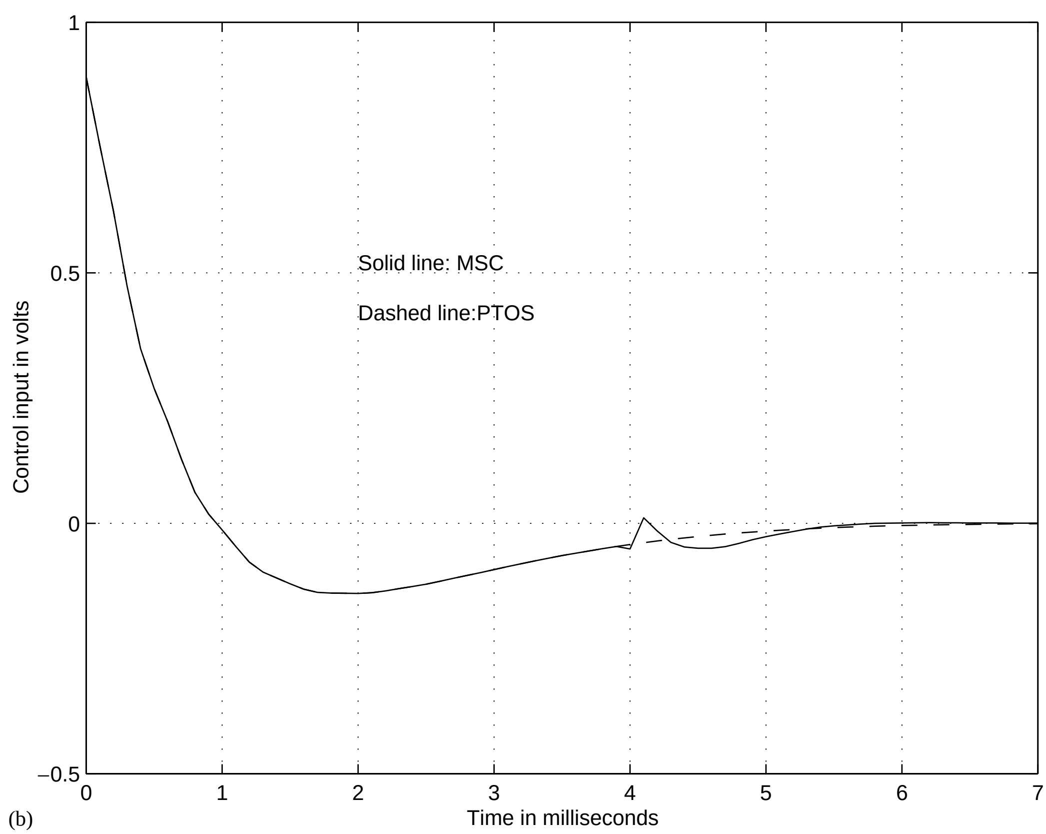

(b)

Fig. 6. Simulation results: response and control for 50 μm displacement: (a) Output responses; (b) control signals.

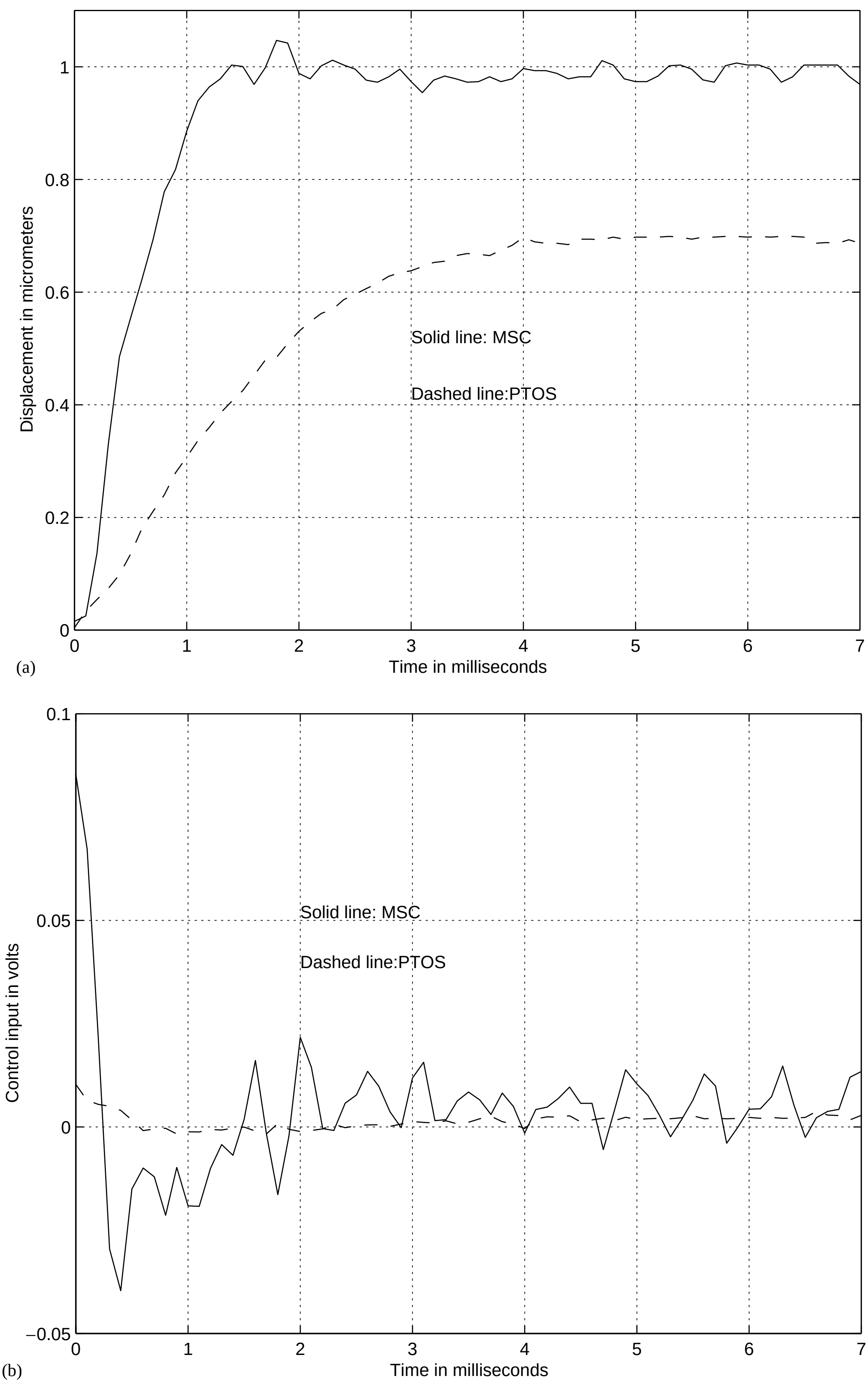


Fig. 7. Implementation results: response and control for 1 μm displacement: (a) Output responses; (b) control signals.

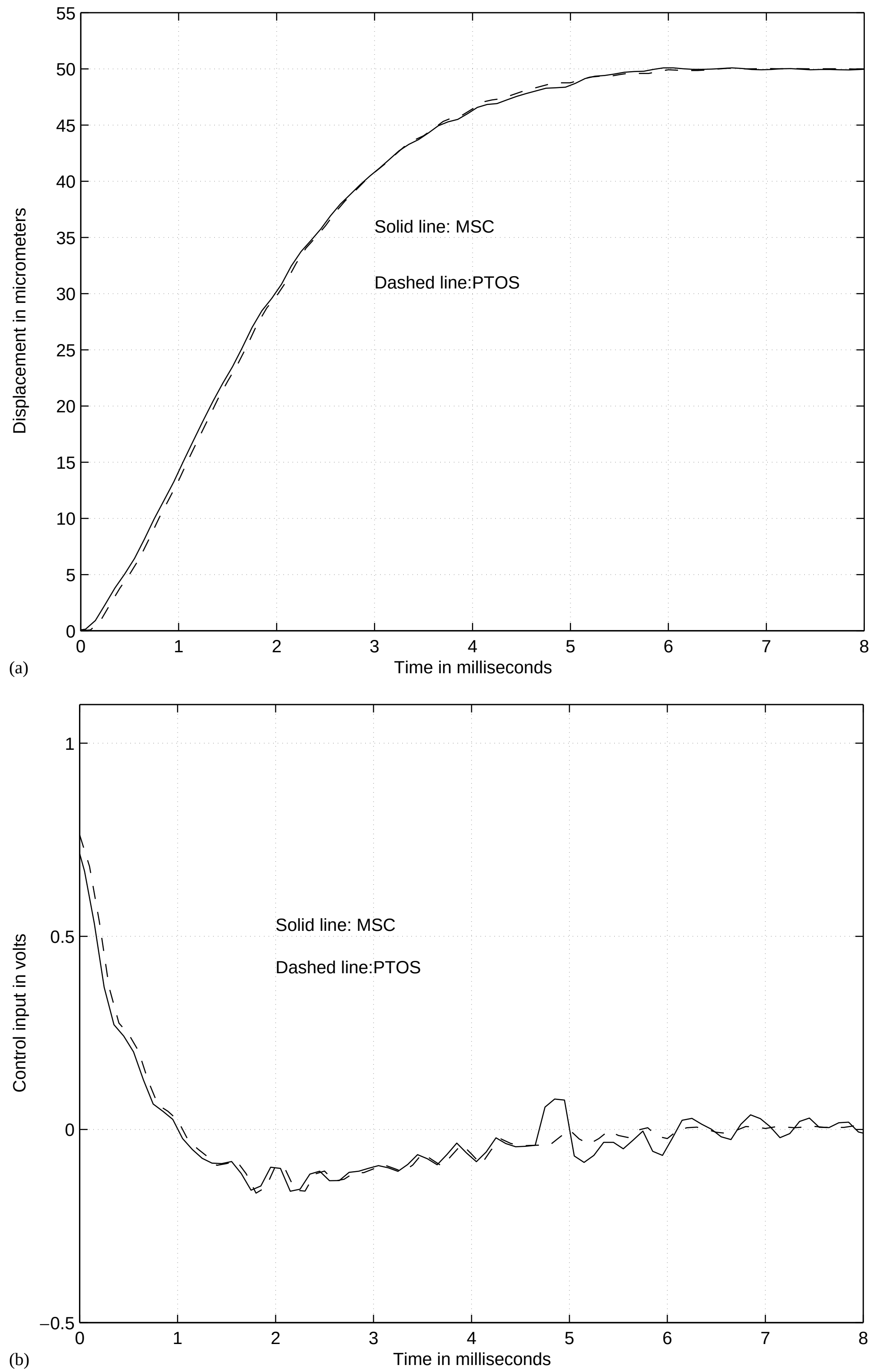


Fig. 8. Implementation results: response and control for 50 μm displacement: (a) Output responses; (b) control signals.

Table 1
Simulation (SIM) and implementation (IMP): settling time and improvment

| Seek length (μm) | Settling times (ms) | | | | Percentage of improvement vs PTOS | |
|---|---|---|---|---|---|---|
| | SIM | | IMP | | | |
| | PTOS | MSC | PTOS | MSC | SIM | IMP |
| 1 | 3.75 | 1.10 | — | 1.25 | 71% | — |
| 50 | 5.45 | 4.90 | 6.50 | 6.00 | 10% | 8% |

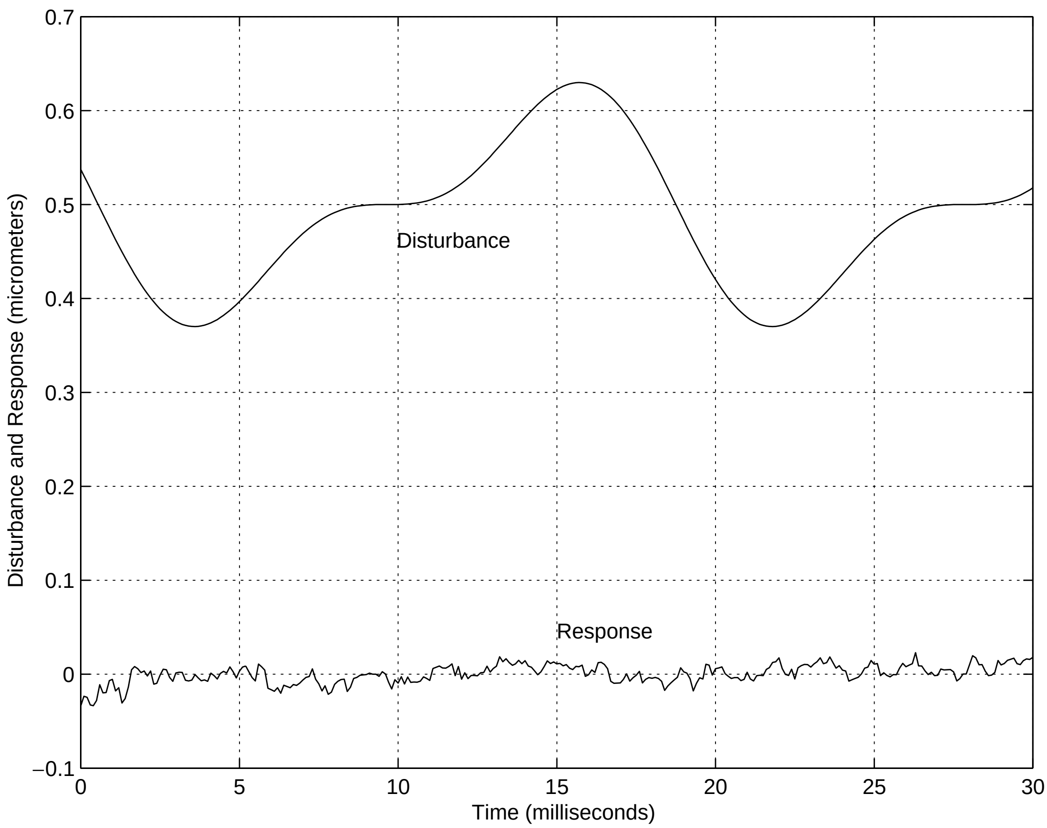


Fig. 9. Implementation result: response to a runout disturbance (MSC).

noise. NRRO are usually random and unpredictable by nature, unlike repeatable runouts. They are also of a lower magnitude (see, e.g., Franklin et al., 1998). A perfect servo system of HDDs should reject both the RRO and NRRO.

Although we do not consider the effects of runout disturbances in our problem formulation, it turns out that our controller is capable of rejecting the first few modes of the runout disturbances, which are mainly due to the imperfectness of the data tracks and the spindle motor speeds, and commonly have frequencies at the multiples of about 55 Hz. In our experiment, we have simplified the system somewhat by removing many sources of disturbances, especially that of the spinning magnetic disk. Therefore, we have to actually add the runouts and other disturbances into the system manually, i.e., the new measurement output is the sum of the actuator output and the runout disturbance. Fig. 9 shows the implementation result of the output response of the overall closed-loop system comprising the actual HDD and the MSC controller with a fictitious runout disturbance injection

$$\tilde{w}(t) = 0.5 + 0.1\cos(110\pi t) + 0.05\sin(220\pi t) \qquad (60)$$

and a zero reference $r(t)$. The result shows that the effects of such a disturbance to the overall response are minimal. Finally, a more comprehensive test on runout disturbances, i.e., the PES test on the actual system is presented.

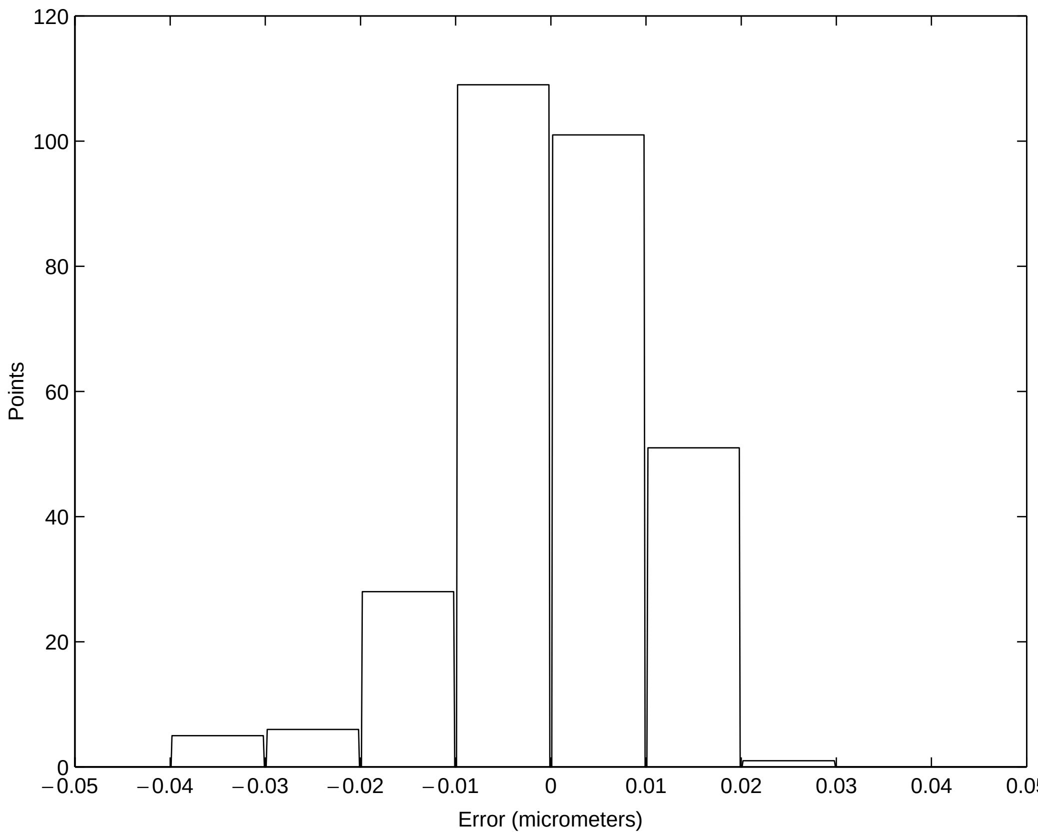


Fig. 10. Implementation result: histogram of PES test (MSC).

### 5.3. Position error signal test

Based on previous experiments, we know that the runouts in real disk drives are mainly composed of the RRO, which is basically sinusoidal with a frequency of about 55 Hz, equivalent to the spin rate of the spindle motor. By manually adding this ‘‘noise’’ to the output while keeping the reference signal to zero, we can then read off the subsequent position signal as the expected PES in the presence of runouts. In disk drive applications, the variations of the R/W head from the center of track during track following, which can be directly read off as the PES, is very important. Track following servo systems have to ensure that the PES is kept to a minimum. Having deviations that are above the tolerance of the disk drive would result in too many read and/or write errors, making the disk drive unusable. A suitable measure is the standard deviation of the readings, $\sigma_{pes}$. A useful guideline is to make the $3\sigma_{pes}$ value $<10\%$ of the track pitch, which is about 0.1 μm for a track density of 25 kTPI (kilo tracks per inch). Fig. 10 shows the histograms of the PES tests for the servo systems with the MSC control law. The $3\sigma_{pes}$ value of the PES test is 0.0306.

## 6. Concluding remarks

We have proposed in this paper a new method for designing HDD servo systems. The proposed method combines two different controllers via a new mode switching technique, which improves the total servo access time. Our simulation and implementation results show that this scheme has improved the overall access time by about 10% for a typical commercially available HDD.


## Acknowledgements

The authors would like to thank Dr. Kemao Peng of the National University of Singapore for many helpful discussions and his assistance in obtaining the experimental results.


## References


Chang, J. K., & Ho, H. T. (1999). LQG/LTR frequency loop shaping to improve TMR budget. *IEEE Transactions on Magnetics*, *35*, 2280–2282.

Chen, B. M. (2000). *Robust and $H_\infty$ control*. London: Springer.

Chen, R., Guo, G., Huang, T., & Low, T. S. (1998). Adaptive multirate control for embedded HDD servo systems. *Proceedings of the 24th annual conference of the IEEE industrial electronics society*, Aachen, Germany (pp. 1716–1720).

Eykhoff, P. (1981). *System identification: Parameter and state estimation*. New York: Wiley.

Franklin, G. F., Powell, J. D., & Workman, M. L. (1998). *Digital control of dynamic systems* (3rd ed.). Reading, MA: Addison-Wesley.

Fujimoto, H., Hori, Y., Yarnaguchi, T., & Nakagawa, S. (2000). Proposal of seeking control of hard disk drives based on perfect tracking control using multirate feedforward control. *Proceedings of the sixth international workshop on advanced motion control*, Nagoya, Japan (pp. 74–79).

Goh, T. B., Li, Z., Chen, B. M., Lee, T. H., & Huang, T. (2001). Design and implementation of a hard disk drive servo system using robust and perfect tracking approach. *IEEE Transactions on Control Systems Technology*, *9*(2), 221–233.

Gu, Y., & Tomizuka, M. (2000). Digital redesign and multi-rate control for motion control—a general approach and application to hard disk drive servo system. *Proceedings of the sixth international workshop on advanced motion control*, Nagoya, Japan (pp. 246–251).

Hanselmann, H., & Engelke, A. (1988). LQG-control of a highly resonant disk drive head positioning actuator. *IEEE Transactions on Industrial Electronics*, *35*, 100–104.

Hara, S., Hara, T., Yi, L., & Tomizuka, M. (1999). Two degree-of-freedom controllers for hard disk drives with novel reference signal generation. *Proceedings of the 1999 American control conference*, San Diego, CA (pp. 4132–4136).

Huang, Y., Messner, W. C., & Steele, J. (1997). Feed-forward algorithms for time-optimal settling of hard disk drive servo systems. *Proceedings of the 23rd international conference on industrial electronics control and instrumentation*, New Orleans, Louisiana (pp. 52–57).

Ishikawa, J., & Tomizuka, M. (1998). A novel add-on compensator for cancellation of pivot nonlinearities in hard disk drives. *IEEE Transactions on Magnetics*, *34*, 1895–1897.

Itkis, U. (1976). *Control systems of variable structure*. New York: Wiley.

Iwashiro, M., Yatsu, M., & Suzuki, H. (1999). Time optimal track-to-track seek control by model following deadbeat control. *IEEE Transactions on Magnetics*, *35*, 904–909.

LaSalle, J. (1961). *Stability by Liapunov's direct method with applications*. New York: Academic Press.

Liu, K., Chen, B. M., & Lin, Z. (2001). On the problem of robust and perfect tracking for linear systems with external disturbances. *International Journal of Control*, *74*(2), 158–174.

Wang, L., Yuan, L., Chen, B. M., & Lee, T. H. (1998). Modeling and control of a dual actuator servo system for hard disk drives. *Proceedings of the 1998 international conference on mechatronic technology*, Hsinchu, Taiwan (pp. 533–538).

Weerasooriya, S., & Phan, D. T. (1995). Discrete-time LQG/LTR design and modeling of a disk drive actuator tracking servo system. *IEEE Transactions on Industrial Electronics*, *42*, 240–247.

Workman, M. L. (1987). *Adaptive proximate time optimal servomechanisms*. Ph.D. Thesis, Stanford University.

Yamaguchi, T., Numasato, H., & Hirai, H. (1998). A mode-switching control for motion control and its application to disk drives: Design of optimal mode-switching conditions. *IEEE/ASME Transactions on Mechatronics*, *3*, 202–209.

Yamaguchi, T., Soyama, Y., Hosokawa, H., Tsuneta, K., & Hirai, H. (1996). Improvement of settling response of disk drive head positioning servo using mode switching control with initial value compensation. *IEEE Transactions on Magnetics*, *32*, 1767–1772.